Proceedings of the XVIII ECSMGE 2024
GEOTECHNICAL ENGINEERING CHALLENGES
TO MEET CURRENT AND EMERGING NEEDS OF SOCIETY

ISBN 978-1-032-54816-6
DOI 10.1201/9781003431749-94

ECSMGE 24
XVIII EUROPEAN CONFERENCE ON SOIL MECHANICS AND GEOTECHNICAL ENGINEERING

Discrete modelling of stress relaxation in crushable sands based on fracture theory

Modélisation discrète de la relaxation des contraintes dans les sables concassés basée sur la théorie de la fracture

J. Lei*, M. Arroyo
Department of Geotechnical Engineering and Geosciences, Polytechnic University of Catalonia (UPC), Barcelona, Spain

M.O. Ciantia
School of Science and Engineering, University of Dundee, Dundee, UK
Università Degli Studi di Milano Bicocca, Milan, Italy

N. Zhang
Institute of Geomechanics and Underground Technology, RWTH Aachen University, Aachen, Germany

**jiangtao.lei@upc.edu*

ABSTRACT: Stress relaxation of quartz sand is simulated using a recently proposed physically based time-to-fracture discrete element method (DEM) framework. The relaxation of stress on sands under high confining pressure is modelled using stress-corrosion induced grain fracture. This feature is embedded into a pre-existing particle-splitting based rough crushable model for Fontainebleau sand. A controlled on-off computational strategy is adopted to advance the simulation. The computed oedometer stress relaxation curve compares favourably with previous experimental results. Triaxial stress relaxation results indicate that stress relaxation increases linearly with time. Contact forces become more homogenous during stress relaxation; as a result, the sample becomes more stable. These microscopic behaviours agree with some observations in pile ageing, suggesting that the model may be adopted directly to investigate such engineering scale phenomena due to its conceptual simplicity, computational efficiency and ease of calibration.

RÉSUMÉ: La relaxation des contraintes du sable de quartz est simulée à l'aide d'un cadre de méthode des éléments discrets (DEM) récemment proposé, basé sur la physique. La relaxation des contraintes sur les sables soumis à une pression de confinement élevée est modélisée à l'aide de la fracture des grains induite par la corrosion sous contrainte. Cette fonctionnalité est intégrée dans un modèle broyable brut préexistant basé sur la division des particules pour le sable de Fontainebleau. Une stratégie de calcul marche-arrêt contrôlée est adoptée pour faire avancer la simulation. La courbe de relaxation des contraintes calculée par l'œdomètre se compare favorablement aux résultats expérimentaux précédents. Les résultats de la relaxation des contraintes triaxiales indiquent que la relaxation des contraintes augmente linéairement avec le temps. Les forces de contact deviennent plus homogènes lors de la relaxation des contraintes; en conséquence, l'échantillon devient plus stable. Ces comportements microscopiques sont en accord avec certaines observations sur le vieillissement des pieux, suggérant que le modèle peut être adopté directement pour étudier de tels phénomènes à l'échelle technique en raison de sa simplicité conceptuelle, de son efficacité de calcul et de sa facilité d'étalonnage.

Keywords: Stress relaxation; discrete-element-modelling; particle crushing; time dependence.

1 INTRODUCTION

Sand stress relaxation is observed when stress decreases under zero deformation. Circumferential stress relaxation, which may strengthen the radial stress along the pile shaft, has been long regarded as one of the most plausible reasons for pile aging (Axelsson, 2000). At high stress levels grain breakage is at root of sand stress relaxation (Lade and Karimpour, 2013).

Current laboratory observations include oedometric stress relaxation tests (Levin et al., 2021) and triaxial stress relaxation tests (Pham Van Bang et al., 2007; Lade and Karimpour, 2015). Different from oedometric stress relaxation where deformation is nil, triaxial stress relaxation is observed by just keeping the axial strain constant under constant cylindrical stress conditions. A linear relationship between the deviatoric stress relaxation and log scale time was observed in those tests.

The discrete element method (DEM) is a very useful tool to find grain-scale explanations of specimen-scale observations. However, as an explicitly advancing method, DEM computation timesteps are always below 1 μs, leading to an overwhelming computational cost for simulating stress relaxation experiments lasting hours to even years. To overcome this difficulty, Wang and Xia (2021), using a rate process theory (RPT) model to simulate stress relaxation in granular materials, scaled up the model viscous parameters by very large numbers to accelerate the simulation. The model is then hard to apply to engineering scale since those scaled parameters lack a clear physical basis and are directly calibrated on specimen-scale responses.

Another option for simulating stress relaxation in sand is based on grain fracture. Xu et al. (2018) adopt a fracture based DEM model to simulate stress relaxation of granular materials. Time advancing is achieved using an on-off computation strategy: a strength ageing model to advance time and DEM dynamic computation only switched on when model equilibrium is required. Xu et al. (2018) used bonded agglomerates, which strongly limits the number of particles in the model, and calibrated parameters on specimen-scale.

In this work we use a time-to-fracture rough crushable DEM sand model to simulate stress relaxation. The model is physically based, computationally efficient and easy to calibrate.

2 MODEL DESCRIPTION

A rough surface Hertzian contact model proposed by Otsubo et al. (2017) was incorporated into the Fontainebleau sand crushable model in Ciantia et al. (2019) by Zhang et al. (2021), to achieve the simulation of mechanical behaviour and accompanied grain sized evolution of real Fontainebleau NE34 sand. The particle strength dominated failure criterion of the model is described in Equation (1):

$$F_n \leq \sigma_{lim,0} \left(\frac{d}{d_0}\right)^{\frac{-3}{m}} f(var)\pi r'\delta \qquad (1)$$

where F_n is the contact normal force, the right hand side of equation is limit force F_{lim}, and it includes two parts: particle strength is $\sigma_{lim,0} \left(\frac{d}{d_0}\right)^{\frac{-3}{m}} f(var)$, both considering strength variance $f(var)$ and size effect $\left(\frac{d}{d_0}\right)^{\frac{-3}{m}}$ in real quartz sand. $\sigma_{lim,0}$ is particle strength at a reference diameter d_0. $\pi r'\delta$ is Hertz contact area. Detailed means of the parameters are shown in Zhang et al. (2021).

Independent of particle strength dominated failure, A crack propagation model proposed by Lei et al. (2024) is adopted here which is an adapted version of normalized Charles (1958) law to determine the crack velocity:

$$v = v_0 (\frac{\sigma}{\sigma_{lim}})^n \qquad (2)$$

where v is crack velocity, v_0 is the reference velocity (0.1 m/s according to Tapias et al., (2015)). σ is the maximum normal contact stress acting on a particle, σ_{lim} is particle strength, which is already defined in Equation (1). n is the stress corrosion index.

Crack half-length a is updated every time interval Δ_t as:

$$a = a_0 + v \times \Delta_t \qquad (3)$$

where a_0 is the initial crack length seeded into each particles following a random uniform distribution ranging from $0.001d$ to $0.5d$, and d is particle diameter.

When $F_n > F_{\text{lim}}$ or $a > 0.5d$, the particle splits into 14 particles, and of which the local axis rotates to direction of normal component of maximum contact force.

Details on the particle splitting mechanism and calibration procedure for the rough crushable time-to-fracture model are given in Zhang et al. (2021) and Lei et al. (2023). Calibrated parameters are presented in Table 1.

Table 1. Model parameters for Fontainebleau sand REV (Lei et al. 2023).

Category	Parameter/unit	Value
Particle failure criteria	G/GPa	32
	ν	0.19
	μ	0.275
	m	12
	$\sigma_{lim,0}$/GPa	3.75
	var	0.38
	d_c/d_{50}	0.55
	d_{max}/mm	0.27
	d_{min}/mm	0.01
Contact roughness	S_q/μm	0.6
	n_1	0.05
	n_2	5
Crack Propagation	v_0	0.1
	n	60

Note: G=shear modulus; ν = Poisson's ratios; μ = interparticle friction coefficient; dc= particle comminution limit; d_{50}=50% pass particle size; d_{max}, d_{min}=maximum, minimum particle diameter; S_q=particle surface roughness; n_1, n_2= roughness parameters.

2.1 Off-DEM ageing

Off-DEM ageing is a strategy to advance time during DEM simulation since the extreme small timestep (below 10^{-6} s) makes impossible continuous simulation of experiments lasting hours to days. The details of Off-DEM ageing are described in Lei et al. (2023, 2024). The simulation begins with a dynamic computation with all model features activated, lasting at least 150,000 cycles. Then it switches to Off-DEM ageing, where only particle crack growth is activated, at a constant velocity given by that at the end of the previous dynamic computation. Potential broken particles during off-DEM (N_{break}) are counted, and once this number reaches a target (in this work N_{break} = 30), dynamic computation is switched on again to break those particles. Those two steps are carried out alternately until the target relaxation time is reached.

3 STRESS RELAXATION SIMULATION

A Fontainebleau sand (quartz) representative element volume (REV) cube containing 11500 particles, of 4mm side with target void ration of 0.65 was formed in PFC3D 5.00.40. Stress relaxation servo-control was achieved by rigid wall motion, setting as boundaries of the REV cube.

3.1 Oedometric stress relaxation

Oedometric stress relaxation with initial vertical stress of 7.5 MPa was carried out to compare with the laboratory results of medium dense sand. Stress during relaxation is normalized by the value at 4s. An acceptable agreement can be observed even if the rough-crushing contact model was initially calibrated to represent a different sand. For the simulation curve, red dots correspond to the periods of dynamic computation, and the time between two red dots is the off-DEM ageing time.

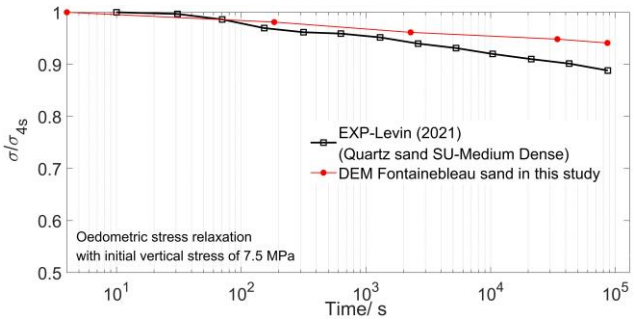

Figure 1. Comparison of DEM model stress relaxation and laboratory results for medium dense quartz sand.

3.2 Triaxial stress relaxation

Triaxial stress relaxation tests were carried out at a high confining pressure of 10 MPa to ensure the sample is in a particle breakage dominated state. Triaxial shearing to failure (30% deviatoric stain) of REV was carried out first to find out the maximum deviatoric stress q_{max} (22.6 MPa). Then stress relaxation tests were conducted maintaining mobilized strength (q/q_{max} = 0.7) for 1 day.

Taking the 4th dynamic computation of triaxial stress relaxation as an example (which denotes the 4th data point in Figure 3), the fluctuation of confining pressure and generated volumetric strain due to previous off-DEM ageing is shown in Figure 2. Figure 2(a) indicates that the confining pressure fluctuation remains a low value during stress relaxation, and Figure 2(b) indicates that although the triaxial stress relaxation accompanying with the generation volumetric strain, the strain remains moderate. These results indicate that dynamic disruption generated by off-DEM ageing remains moderate, and that the control value (N_{break} = 30) in switching to DEM is appropriate (see also Lei et al. (2023), for a parametric study on N_{break}).

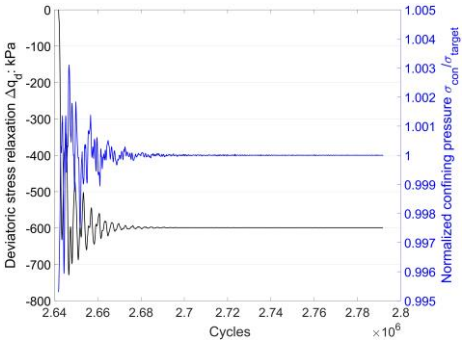

(a)

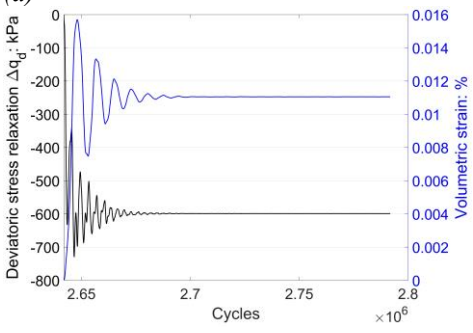

(b)

Figure 2. Confining pressure fluctuation(a) and generated volumetric strain (b) during 4th dynamic computation of triaxial stress relaxation.

Figure 3 shows the simulated triaxial stress relaxation with time. A linear relationship can be observed, and similar relaxation trends were also

observed in Lade and Karimpour (2015) and Pham Van Bang et al. (2007) for quartz sands.

Figure 4 shows the standard deviation evolution of normal contact forces F_n and tangential contact forces F_t during stress relaxation. A decreasing trend can be observed for all cases, indicating how stress relaxation homogenizes contact forces. The similar stress homogenization was also observed by Zhang and Wang (2015) for Toyoura sand around pile after pile set-up, in which they adopt tiny sensing elements to measure the normal contact stresses.

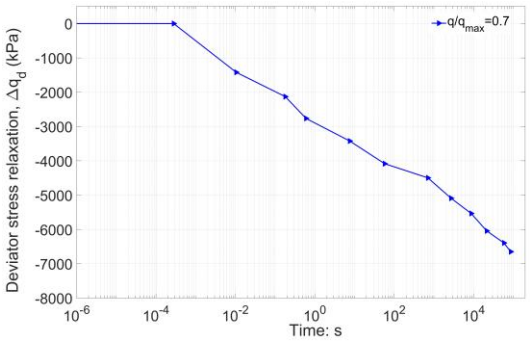

Figure 3. Triaxial stress relaxation with time in DEM simulation.

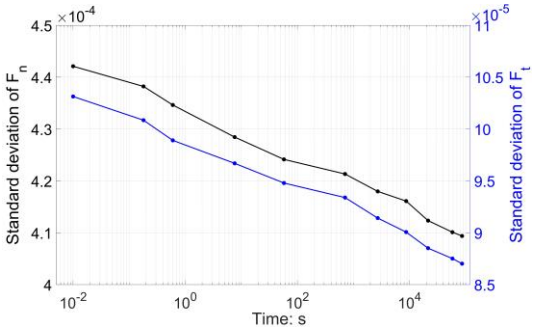

Figure 4. Standard deviation evolution of (a) normal contact forces (b)tangential contact forces.

4 CONCLUSIONS

A fracture based rough crushable Fontainebleau sand DEM model is applied here to simulate stress relaxation, and a good agreement with laboratory results of quartz sands can be found. Contact forces homogenization during relaxation indicates the possible association between stress relaxation and pile set-up.

ACKNOWLEDGEMENTS

The first author is supported by Chinese Government Scholarship CSC (No.202108390006). Spanish Research Agency support (AEI) through research project PID2020-119598RB-I00 is also acknowledged.

REFERENCES

Axelsson, G. (2000). "Long-term set-up of driven piles in sand." Ph.D. thesis, Royal Institute of Technology, Stockholm, Sweden.

Charles, R. J. (1958). Static fatigue of glass. *Journal of Applied Physics* 29(11): 1549–1560.

Ciantia, M. O., Arroyo, M., O'Sullivan, C., Gens, A., and Liu, T. (2019). Grading evolution and critical state in a discrete numerical model of Fontainebleau sand. *Geotechnique*, *69*(1): 1–15. https://doi.org/10.1680/jgeot.17.P.023.

Lade, P. v., and Karimpour, H. (2015). Stress relaxation behavior in Virginia Beach sand. *Canadian Geotechnical Journal*, *52*(7): 813–835. https://doi.org/10.1139/cgj-2013-0463.

Lei, J., Arroyo, M., Ciantia, M. and Zhang, N. (2023) A time-to-fracture DEM model for simulating creep in rough crushable sand.*10th European Conference on Numerical Methods in Geotechnical Engineering, London, UK.* https:// 10.53243/NUMGE2023-37.

Lei, J., Arroyo, M., Ciantia, M., & Zhang, N. (2024). A fracture-based discrete model for simulating creep in quartz sands. *Géotechnique*, 1–43. https://doi.org/10.1680/jgeot.23.00068.

Levin, F. (2021). Time-Dependent Compression Behavior of Sands under Oedometric Conditions. *J. Geotech. Geoenviron.*, *147*(12). https://doi.org/10.1061/(ASCE)GT.1943-5606.0002664.

Otsubo, M., O'Sullivan, C., Hanley, K. J., and Sim, W. W. (2017). The influence of particle surface roughness on elastic stiffness and dynamic response. *Geotechnique*, *67*(5): 452–459. https://doi.org/10.1680/jgeot.16.P.050.

Pham Van Bang, D., di Benedetto, H., Duttine, A., & Ezaoui, A. (2007). Viscous behaviour of dry sand. *Int. J Numer. Anal. Met*, *31*(15): 1631–1658. https://doi.org/10.1002/nag.606..

Tapias, M., Alonso, E. E., and Gili, J. (2015). A particle model for rockfill behaviour. *Geotechnique*, *65*(11): 975–994. https://doi.org/10.1680/jgeot.14.P.170.

Wang, J., and Xia, Z. (2021). DEM study of creep and stress relaxation behaviors of dense sand. *Computers and Geotechnics*, *134*. https://doi.org/10.1016/j.compgeo.2021.104142.

Xu, M., Hong, J., and Song, E. (2018). DEM study on the macro- and micro-responses of granular materials subjected to creep and stress relaxation. *Computers and Geotechnics*, *102*: 111–124. https://doi.org/10.1016/j.compgeo.2018.06.009.

Zhang, N., Ciantia, M. O., Arroyo, M., and Gens, A. (2021). A contact model for rough crushable sand. *Soils and Foundations* 61(3): 798–814. https://doi.org/10.1016/j.sandf.2021.03.002.

Zhang, Z., and Wang, Y. H. (2015). Examining Setup Mechanisms of Driven Piles in Sand Using Laboratory Model Pile Tests. *Journal of Geotechnical and Geoenvironmental Engineering*, *141*(3). https://doi.org/10.1061/(ASCE)GT.1943-5606.0001252.